

Electric-field-induced wetting and dewetting in single hydrophobic nanopores

Matthew R. Powell¹, Leah Cleary², Matthew Davenport¹, Kenneth J. Shea² and Zuzanna S. Siwy^{1*}

The behaviour of water in nanopores is very different from that of bulk water^{1,2}. Close to hydrophobic surfaces, the water density has been found to be lower than in the bulk³, and if confined in a sufficiently narrow hydrophobic nanopore, water can spontaneously evaporate⁴. Molecular dynamics simulations have suggested that a nanopore can be switched between dry and wet states by applying an electric potential across the nanopore membrane^{5–8}. Nanopores with hydrophobic walls could therefore create a gate system for water, and also for ionic and neutral species. Here, we show that single hydrophobic nanopores can undergo reversible wetting and dewetting due to condensation and evaporation of water inside the pores. The reversible process is observed as fluctuations between conducting and non-conducting ionic states and can be regulated by a transmembrane electric potential.

So far, hydrophobic man-made nanoporous systems have consisted of multipore membranes that transport water solutions when a pressure difference is applied across them⁹. Hydrophobic nanopores with diameters less than 50 nm require pressures of tens of atmospheres to allow water and ionic transport. Making use of a transmembrane electric potential offers an attractive alternative to pressure-driven transport as it does not require the system to be highly mechanically robust—either inherently or through supports—and it can therefore be applicable to a wider variety of nanopore platforms, including biological channels in lipid bilayers. The suggested physical mechanism of the electric-field wetting effect is based on orienting water dipoles in the field and water electrostriction (that is, increase in water density) in the hydrophobic regions, which ultimately leads to a pore filling with liquid water^{6,7,10}. The process of wetting/dewetting via the hydrophobic lining of the pore walls has also been recognized as a key mechanism for the function of bacterial mechano-sensitive biological channels¹¹ as well as a wide family of voltage-gated channels in which the existence of a conserved hydrophobic region has recently been reported¹². Formation of nanobubbles in the pore lumen has also been suggested as a possible mechanism for ion channel gating¹³.

The main challenge in building a hydrophobic valve is the ‘drying’ (through water evaporation) of the once wet pores on removal of the stimulus. Almost all hydrophobic membranes reported to date are one-time devices: once wetted, they remain filled with water and allow mass transport¹⁴. Only one recent report¹⁰ has demonstrated the ability of hydrophobic SiN pores to reversibly switch between low and high conductance states. However, the low conductance state still exhibited a finite ion current, probably because of the relatively large pore opening diameter (between 60 and 600 nm) and small thickness (300 nm) of the SiN pores¹⁰. Dewetting of nanopores is thermodynamically favourable for a wide range of nanopore diameters, but has been predicted to be kinetically feasible only in nanopores several nanometres in diameter^{15–17}. In our experiments, which were performed with long nanopores (two to four orders of

magnitude longer than those used in previous simulations^{16,17} and experiments¹⁰), we observed spontaneous wetting (finite conductance) and dewetting (zero conductance) processes recorded as ion current fluctuations in pores with diameters up to ~20 nm. Furthermore, the process could be regulated by applying an external voltage in the range 0–10 V.

Single conically shaped nanopores were prepared in 12- μ m-thick films of polyethylene terephthalate (PET) using a track-etching technique^{18,19}. The large opening of the studied pores was ~500 nm in diameter, and the small opening was between 4 and ~30 nm. As a result of the pore fabrication technique, the pore walls contained carboxyl groups at a density of ~1 nm⁻²; these render the pores hydrophilic and allow them to be filled easily with an electrolyte solution. A nanometre opening of the as-prepared nanopores was confirmed by observing rectifying properties of the structures in 0.1 M KCl solution (pH 8), in which the carboxyl groups were deprotonated^{19–21}. The carboxyl groups also allowed methyl groups to be grafted onto the pore walls by treatment of the membranes with (trimethylsilyl)diazomethane in methanol to provide methyl esters. The success of the reaction was confirmed by measuring the contact angle of a planar PET etched surface that was subjected to the same chemical modification as the single nanopores. An etched PET surface is characterized by a contact angle of ~60°, but overnight reaction in 200 mM (trimethylsilyl)diazomethane results in a hydrophobic surface characterized by a contact angle of ~102°. The hydrophobic character of the surface arises because of the introduced methyl groups as well as the exposed aromatic groups of the polymer structure.

The transport properties of the modified pores were studied as a function of modification time and (trimethylsilyl)diazomethane concentration (Supplementary Table S1). Modification of the pore walls for short reaction times at dilute concentrations of (trimethylsilyl)diazomethane (0.1–12 mM) induced voltage-dependent ionic transport through the structures, which was studied by recording 2-min-long ion-current time series. Averaging the time series resulted in current–voltage curves that allowed for a quick assessment of the voltage sensitivity of the pores (Fig. 1a). Figure 1 shows the ion current through a nanopore with a narrow opening (diameter, 16 nm) that was modified with 12 mM (trimethylsilyl)diazomethane for 15 min. For voltages below 1 V, the pore was mostly closed and no current was recorded. At ~2 V the pore opened, and bursts of large-amplitude current signals of several nanoamperes could be observed. The bursts became more frequent at higher voltages and eventually, at +5 V, the pore remained in the open state (Fig. 1c). The voltage-dependent enabling of ionic transport did not always induce the quick kinetic opening and closing as is shown for positive voltages in Fig. 1. When negative voltages were applied (Fig. 1d), the same pore opened and closed on a much slower timescale, to the extent that the pore would stay in the open state for up to tens of seconds.

¹Department of Physics and Astronomy, University of California, Irvine, California 92697, USA, ²Department of Chemistry, University of California, Irvine, California 92697, USA. *e-mail: zsiwy@uci.edu

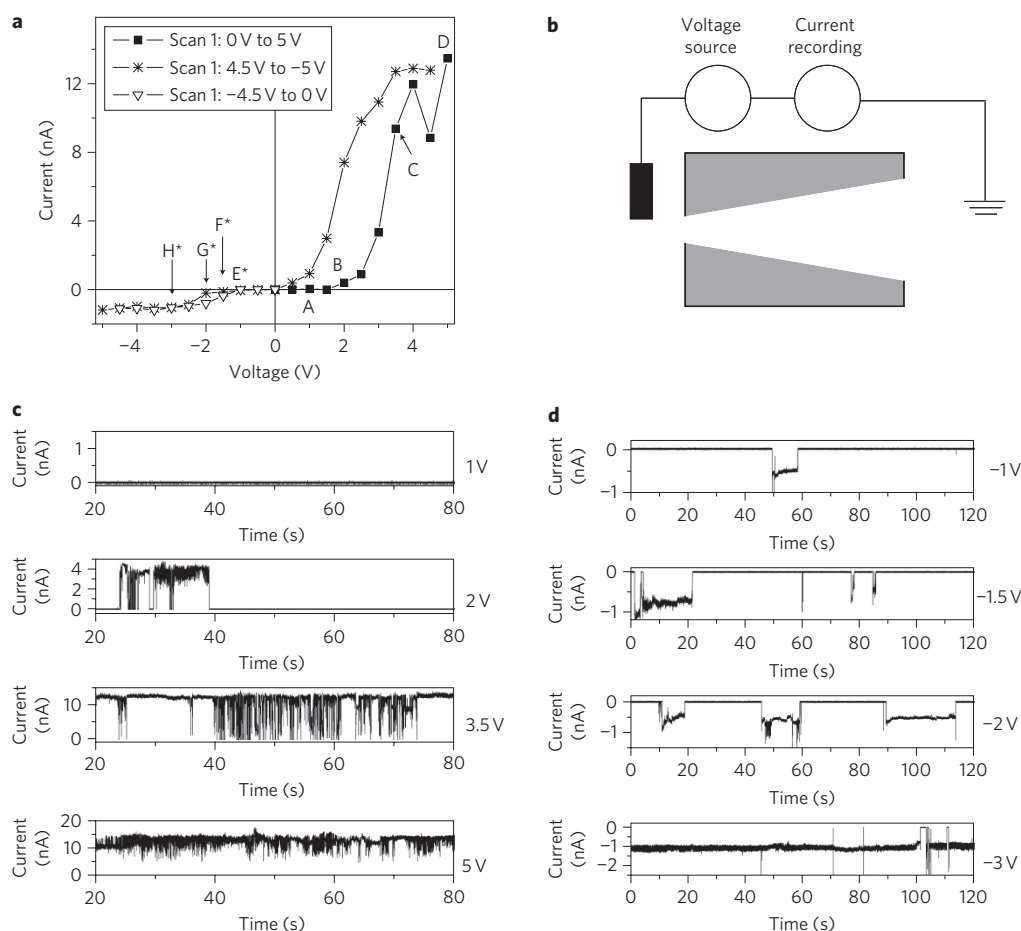


Figure 1 | Hydrophobic gating in a 16-nm-diameter conically shaped nanopore modified in 12 mM (trimethylsilyl)diazomethane for 15 min. **a, b,** Current-voltage characteristic (**a**) obtained by averaging 2-min ion-current time series, with the voltage (**b**) changed in steps of 0.5 V from 0 V to +5 V, followed by a sweep from +4.5 V to -5 V and from -4.5 V to 0 V. **c,** Example recordings for positive voltages. **d,** Example ion current series for negative voltages. Quick opening and closing kinetics were observed for positive voltages between 2 V and 4.0 V (time series for 2 V and 3.5 V are shown). For negative voltages the pore stayed in the conducting and non-conducting states for much longer periods, on the order of tens of seconds (recordings at -1 V, -1.5 V, -2 V). All recordings were performed in an as-prepared, non-degassed solution of 1 M KCl, pH 8 (Tris buffer). Letters with asterisks in **a** indicate time series for which averages are marked on the graph with a star. The hysteresis seen for positive voltages was not present in all voltage scans performed for this pore (Fig. 2). In other pores the hysteresis occurred for either of the two voltage polarities (data in Supplementary Information). The pore switching can have two-state or multiple-state character (Supplementary Figs S2-S13).

We would like to emphasize that within the picoampere resolution of our recording system, the non-conducting, closed state was characterized by no current. Such a perfectly non-conducting state is typically obtained only when the two chambers of the conductivity cell are not connected by an electrolyte (for example, when the pore is not filled with the solution or there is no pore in the membrane at all). We propose that the non-conducting state observed with the (trimethylsilyl)diazomethane-modified pores corresponds to the pore or at least a section of the pore being filled with water vapour, whereas the conducting state indicates wetting of the pore along its whole length.

To confirm the reversibility of the pore switching between conducting and non-conducting states the voltage was switched between +1 V when the pore was closed and +5 V, when the pore was expected to open (Fig. 1a,c). Excellent reproducibility of the pore gating and almost instantaneous switching was demonstrated, as shown in Fig. 2a. Additional voltage scans were performed between -5 V and +5 V to obtain data similar to that in Fig. 1 for the same nanopore. Current-voltage curves of two scans are shown in Fig. 2b and confirm the voltage-induced and reversible opening and closing of the pore to ionic transport. The voltage at which the

pore opening occurs changes with each scan; however, the closure of the pore at ~1 V was reproduced (Supplementary Fig. S1).

It is also important to note that the kinetics of the opening and closing of the pores changes with each voltage sweep (Supplementary Figs S2-S13). The fast kinetics of pore switching for some pores appears for opposite voltage polarities and different voltage values (Supplementary Figs S5-S9). In some cases, the pore opening was very abrupt and not preceded by current fluctuations (Supplementary Figs S3-S7).

The data shown in Figs 1 and 2 were obtained with as-prepared (non-degassed) KCl solutions. To evaluate the importance of the dissolved gases in the voltage-gating process³, we also measured ion current with a solution that was degassed in a vacuum chamber for 2 h. Controlled opening and closing of the ion current with voltage was indeed observed with the degassed solution, confirming that the dissolved gases did not play a substantial role in the hydrophobic gating observed in the polymer pores (Fig. 3, Supplementary Figs S4-S6).

Nanopores modified in 200 mM (trimethylsilyl)diazomethane for 2 h and longer did not exhibit any ionic transport with external voltages up to 10 V. The pores were, however, physically open,

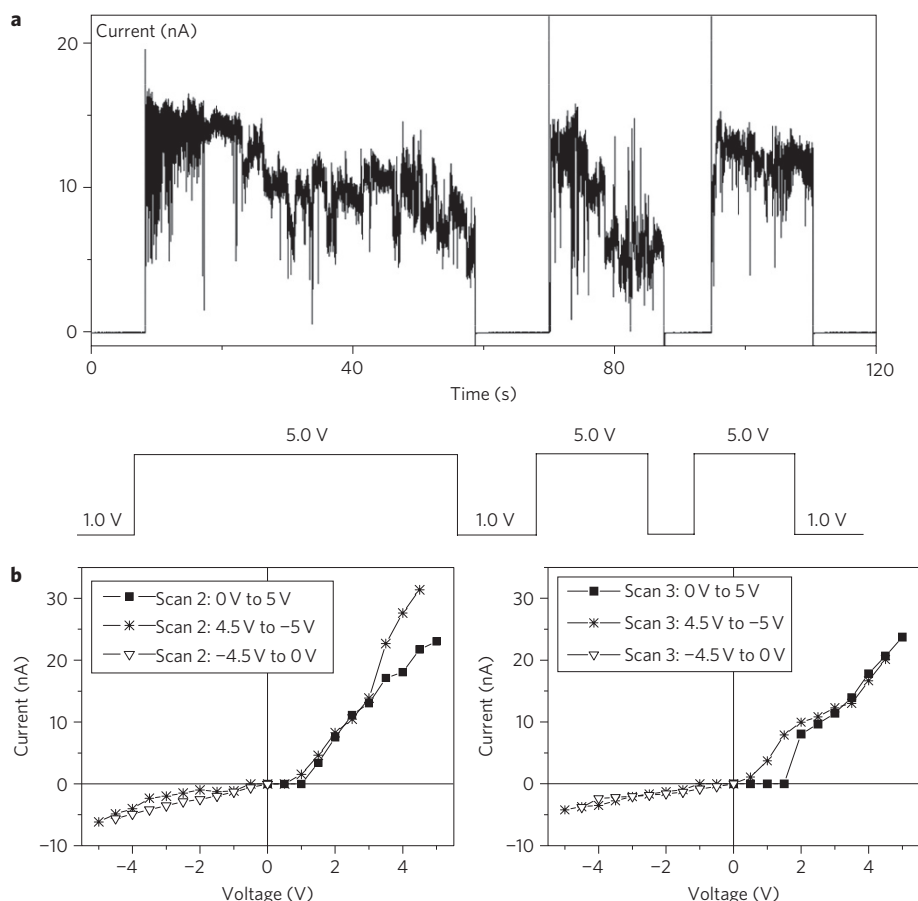


Figure 2 | Reversibility of the opening and closing of a hydrophobic nanopore with voltage. Data were recorded for the same nanopore as in Fig. 1. The pore opening diameter was 16 nm, and the pore was subjected to 15 min modification in 12 mM (trimethylsilyl)diazomethane. **a**, The voltage was manually switched between +1 V and +5 V, leading to reversible switching of the pore between non-conducting and conducting states. **b**, Current-voltage curves obtained by averaging 2-min ion-current series recorded when the voltage was changed in steps of 0.5 V from 0 V to +5 V, followed by a sweep from +4.5 V to -5 V and from -4.5 V to 0 V. Two such voltage scans were performed (Scan 2 and Scan 3) after the data in Fig. 1 had been measured. The scans are presented in separate graphs to facilitate comparison of the hysteresis effect. The voltages scans are superimposed as one graph in Supplementary Fig. S1. All recordings were performed in an as-prepared, non-degassed solution of 1 M KCl, pH 8 (Tris buffer).

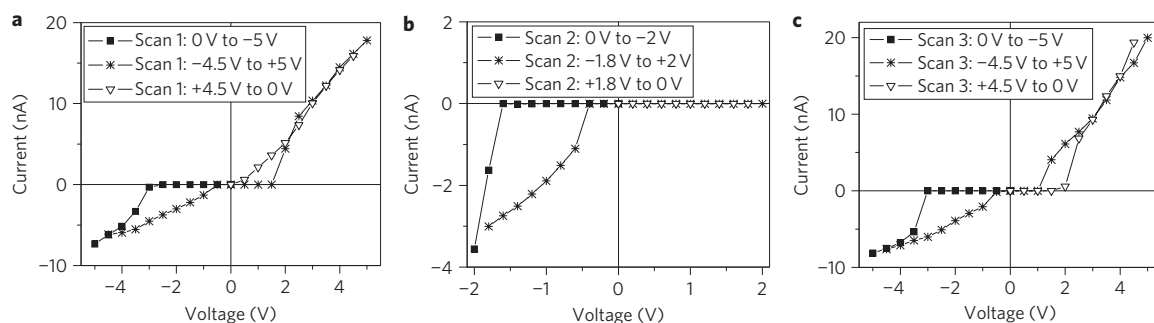


Figure 3 | Hydrophobic gating studied in a degassed solution of 1 M KCl. **a-c**, The potential influence of dissolved gases on the ability of a pore to switch between conducting and non-conducting states was studied in a 16-nm-diameter pore modified in 5 mM (trimethylsilyl)diazomethane for 15 min. Ion current recordings were performed in a 1 M KCl solution that was degassed in a vacuum chamber. The voltage sweeps in **a** (Scan 1) and **c** (Scan 3) were repeated twice with voltage steps of 0.5 V, from 0 V to -5 V, from -4.5 V to +5 V and from +4.5 V to 0 V. Scan 2 (**b**) was performed in the voltage range -2 V to +2 V, in steps of 0.2 V. At each voltage step, the ion-current time series was recorded for 2 min. The presented current-voltage curves were obtained by averaging the ion-current time series. Details of the ion current switching in time are shown in the Supplementary Information.

because washing the pores with ethanol (and quick drying in air) before the introduction of KCl solution into the cell facilitated filling the pores with the electrolyte, and voltage-induced openings and closings (Supplementary Table S1, Figs S14–S16).

The question still remains whether the non-conducting state of our nanopores indeed corresponds to the presence of water vapour. Hydrophobic nanopores were predicted to exhibit a higher barrier to ions than water^{22,23}. A hydrophobic nanopore can therefore

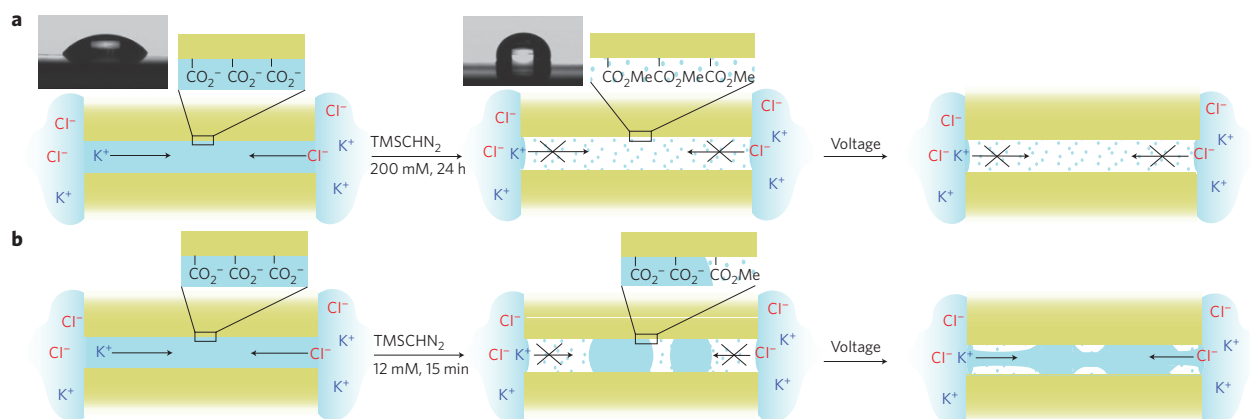


Figure 4 | Scheme of hydrophobic gating with an electric field. **a**, An unmodified PET pore is hydrophilic, as indicated by a contact angle of $\sim 60^\circ$ (image in left panel) measured on a planar surface. Overnight modification of the pores in a concentrated solution of (trimethylsilyl)diazomethane led to homogeneously hydrophobic surfaces with a contact angle of $\sim 102^\circ$ (image in middle panel). **b**, Shorter modifications performed in diluted solutions of (trimethylsilyl)diazomethane led to the formation of less hydrophobic surfaces characterized by contact angles less than 90° (Supplementary Table S2). We propose that local hydrophobic clusters are created, which induce the formation of local vapour pockets. Applying an electric field across the membrane favours filling the pore with water and therefore ionic transport. A small fragment of a polymer nanopore is presented and its shape is approximated by a cylinder.

potentially contain just water, but still no ionic transport will occur. To investigate this, we performed ion current measurements of (trimethylsilyl)diazomethane-modified nanopores in 0.1 M HCl. If the pores contain liquid water along their entire length, then we should see a residual current originating from proton transport due to the Grotthuss mechanism. It is well known that it is difficult to prevent protons from flowing through even a single file of water as occurs in aquaporins²⁴. Supplementary Fig. S18 confirms that no ion current was observed in the (trimethylsilyl)diazomethane-modified nanopores in 0.1 M HCl, which provides evidence that the non-conducting state corresponds to a nanopore either completely or in part filled with water vapour and not liquid water.

Polymer nanopores (diameter, ~ 15 nm) modified with 0.1–12 mM (trimethylsilyl)diazomethane for 15 min exhibited voltage-regulated hydrophobic gating (Fig. 1). Planar PET surfaces subjected to identical modification had contact angles less than 90° (for example, $\sim 75^\circ$ for modification in 12 mM (trimethylsilyl)diazomethane, Supplementary Table S2), indicating that the chemical modification was not complete, forming isolated hydrophobic clusters rather than a completely homogeneous hydrophobic surface (Fig. 4). Thus, water evaporation probably occurs only locally in the hydrophobic regions, which will also create the highest-resistance areas where the applied voltage will primarily drop. Wetting of hydrophobic pores was predicted to occur only when the applied electric field exceeded the threshold value^{8,10}, which is easier to obtain in nanopores with smaller hydrophobic clusters present in pores modified with a lower concentration of (trimethylsilyl)diazomethane. As modelled in refs 25–27, ~ 2 -nm-large hydrophobic clusters, even if immersed in a hydrophilic matrix, are already sufficiently large to induce local water evaporation and the formation of vapour pockets.

In summary, we have reported nanopores with hydrophobic regions that exhibit voltage-dependent wetting and ionic transport. The observed non-conducting state was attributed to the existence of a local region filled with water vapour that created a high-resistance bottleneck to ionic transport. Hydrophobic nanopores and membranes could create an ideal system for controlled material delivery, which without an applied stimulus would not cause any unwanted leakage. In addition, single hydrophobic nanopores allow hydrophobic interactions and water structure to be studied at the nanoscale.

Methods

Preparation of single conical nanopores. Experiments were performed with single conically shaped nanopores embedded in 12- μ m-thick PET films. The pores were prepared by a track-etching technique¹⁸, which entails irradiating a polymer film with single swift heavy ions and subsequent asymmetric etching in concentrated NaOH (ref. 19). The fabrication process leads to the formation of conically shaped nanopores. The diameter of the small opening was estimated based on an electrochemical technique which relates pore resistance to its geometry¹⁹. The large opening of the pore was determined from the rate of non-specific etching of the polymer material, which for PET at room temperature is 2.13 nm min^{-1} .

Chemical modification of polymer pores. Track-etched PET films were placed individually in a flame-dried Erlenmeyer flask purged with N_2 and stoppered with a rubber septum. Freshly distilled MeOH was then added, followed by (trimethylsilyl)diazomethane (2 M in hexanes) to afford the desired concentration. After the requisite reaction time (15 min to 24 h), excess (trimethylsilyl)diazomethane was quenched by the addition of 1 ml of water. The film was then removed from solution, washed successively with MeOH and water ($3 \times 5 \text{ ml}$), and allowed to air dry.

Ion current recordings. Single pore membranes were mounted between two chambers of a conductivity cell characterized by a seal resistance of $\sim 1,000 \text{ G}\Omega$. We used home-made Ag/AgCl electrodes to measure the transmembrane current. The ion current was recorded using an Axopatch 200B amplifier interfaced with a PC via a Digidata 1322A digitizer (Molecular Devices) using the voltage-clamp mode and a sampling frequency of 10 kHz. The signal was subsequently filtered with a 2 kHz low-pass Bessel filter. The external voltage source of the Digidata was used to apply voltages in the range between -10 V and 10 V . The time series of ion current at each voltage was recorded for 2 min. Current–voltage curves were obtained by calculating arithmetic averages of the time recordings.

Received 2 August 2011; accepted 28 September 2011;
published online 30 October 2011

References

- Israelachvili, J. N. *Intermolecular and Surface Forces* (Academic Press, 1991).
- Meyer, E. E., Rosenberg, K. J. & Israelachvili, J. Recent progress in understanding hydrophobic interactions. *Proc. Natl Acad. Sci. USA* **103**, 15739–15746 (2006).
- Doshi, D. A., Watkins, E. B., Israelachvili, J. & Majewski, J. Reduced water density at hydrophobic surfaces: effect of dissolved gases. *Proc. Natl Acad. Sci. USA* **102**, 9458–9462 (2005).
- Lum, K., Chandler, D. & Weeks, J. D. Hydrophobicity at small and large length scales. *J. Phys. Chem. B* **103**, 4570–4577 (1999).
- Vaitheeswaran, S., Rasaiah, J. C. & Hummer, G. Electric field and temperature effects on water in the narrow nonpolar pores of carbon nanotubes. *J. Chem. Phys.* **121**, 7955–7965 (2004).
- Dzubiella, J., Allen, R. J. & Hansen, J.-P. Electric field-controlled water permeation coupled to ion transport through a nanopore. *J. Chem. Phys.* **120**, 5001–5004 (2004).

7. Dzubiella, J. & Hansen, J.-P. Electric-field-controlled water and ion permeation of a hydrophobic nanopore. *J. Chem. Phys.* **122**, 234706 (2005).
8. Bratko, D., Daub, C. D., Leung, K. & Luzar, A. Effect of field direction on electrowetting in a nanopore. *J. Am. Chem. Soc.* **129**, 2504–2510 (2007).
9. Smirnov, S., Vlassioudis, I., Takmakov, P. & Rios, F. Water confinement in hydrophobic nanopores. Pressure-induced wetting and drying. *ACS Nano* **4**, 5069–5075 (2010).
10. Smirnov, S. N., Vlassioudis, I. V. & Lavrik, N. V. Voltage-gated hydrophobic nanopores. *ACS Nano* **5**, 7453–7461 (2011).
11. Sukharev, S. I., Sigurdson, W. J., Kung, C. & Sachs, F. Energetic and spatial parameters for gating of the bacterial large conductance mechanosensitive channel, MscL. *J. Gen. Physiol.* **113**, 525–540 (1999).
12. Jensen, M. Ø. *et al.* Principles of conduction and hydrophobic gating in K⁺ channels. *Proc. Natl Acad. Sci. USA* **107**, 5833–5838 (2010).
13. Roth, R., Gillespie, D., Nonner, W. & Eisenberg, R. E. Bubbles, gating, and anesthetics in ion channels. *Biophys. J.* **94**, 4282–4298 (2008).
14. Vlassioudis, I., Park, C.-D., Vail, S. A., Gust, D. & Smirnov, S. Control of nanopore wetting by a photochromic spiropyran: a light-controlled valve and electrical switch. *Nano Lett.* **6**, 1013–1017 (2006).
15. Leung, K., Luzar, A. & Bratko, D. Dynamics of capillary drying in water. *Phys. Rev. Lett.* **90**, 065502 (2003).
16. Hummer, G., Rasaiah, J. C. & Noworyta, J. P. Water conduction through the hydrophobic channel of a carbon nanotube. *Nature* **414**, 188–190 (2001).
17. Beckstein, O. & Sansom, M. S. P. Liquid-vapor oscillations of water in hydrophobic nanopores. *Proc. Natl Acad. Sci. USA* **100**, 7063–7068 (2003).
18. Fleischer, R. L., Price, P. B. & Walker, R. M. *Nuclear Tracks in Solids. Principles and Applications* (Univ. California Press, 1975).
19. Apel, A., Korchev, Y. E., Siwy, Z., Spohr, R. & Yoshida, M. Diode-like single-ion track membrane prepared by electro-stopping. *Nucl. Instrum. Methods Phys. Res. B* **184**, 337–346 (2001).
20. Siwy, Z. & Fulinski, A. Fabrication of a synthetic nanopore ion-pump. *Phys. Rev. Lett.* **89**, 198103 (2002).
21. Siwy, Z. S. & Howorka, S. Engineered voltage-responsive nanopores. *Chem. Soc. Rev.* **39**, 1115–1132 (2010).
22. Shirono, K., Tatsumi, N. & Daiguji, H. Molecular simulation of ion transport in silica nanopores. *J. Phys. Chem. B* **113**, 1041–1047 (2009).
23. Beckstein, O., Tai, K. & Sansom, M. S. P. Not ions alone: barriers to ion permeation in nanopores and channels. *J. Am. Chem. Soc.* **126**, 14694–14695 (2004).
24. Tajkhorshid, E. *et al.* Control of the selectivity of the aquaporin water channel family by global orientational tuning. *Science* **296**, 525–530 (2002).
25. Giovambattista, N., Debenedetti, P. G. & Rossky, P. J. Hydration behavior under confinement by nanoscale surfaces with patterned hydrophobicity and hydrophilicity. *J. Phys. Chem. C* **111**, 1323–1332 (2007).
26. Parikesit, G. O. F., Vrouwe, E. X., Blom, M. T. & Westerweel, J. Observation of hydrophobic-like behavior in geometrically patterned hydrophilic microchannels. *Biomicrofluidics* **4**, 044103 (2010).
27. Koishi, T., Yasuoka, K., Ebisuzaki, T., Yoo, S. & Zeng, X. C. Large-scale molecular-dynamics simulation of nanoscale hydrophobic interaction and nanobubble formation. *J. Chem. Phys.* **123**, 204707 (2005).

Acknowledgements

Irradiation with swift heavy ions was performed at the Gesellschaft fuer Schwerionenforschung (GSI, Darmstadt, Germany). This research was supported by the National Science Foundation (CHE 0747237). Z.S.S. was supported as part of the Nanostructures for Electrical Energy Storage, an Energy Frontier Research Center funded by the US Department of Energy, Office of Science, Office of Basic Energy Sciences (award no. DESC0001160). The authors acknowledge discussions with C. Martens.

Author contributions

Z.S.S., M.D. and K.J.S. conceived the experiments. M.R.P., L.C. and M.D. performed the experiments. All authors contributed to writing the manuscript. M.R.P., L.C., M.D., K.J.S. and Z.S.S. discussed the results and explained the transient behaviour of ion current in hydrophobic pores.

Additional information

The authors declare no competing financial interests. Supplementary information accompanies this paper at www.nature.com/naturenanotechnology. Reprints and permission information is available online at <http://www.nature.com/reprints>. Correspondence and requests for materials should be addressed to Z.S.S.